International Journal of Mechanical and Production Engineering Research and Development (IJMPERD)
ISSN(P): 2249-6890; ISSN(E): 2249-8001
Vol. 9, Issue 1, Feb 2019, 179-190

AN INVESTIGATION OF ANALYTICAL MODELLING OF FRICTION STIR WELDING

J. STEPHEN LEON & V. JAYAKUMAR

Department of Mechanical Engineering, Saveetha School of Engineering, Saveetha Institute of Medical and Technical Sciences, Chennai, Tamil Nadu, India

ABSTRACT

Weld properties in Friction Stir Welding (FSW)depend on the peak temperature attained during the process and cooling rate. Temperature cycles in this joining process decides the microstructure not only in the weldment but also in the heat affected zones of the parental metal. The complex flow of plasticized metal makes it difficult to measure generated heat directly which results the metal mixing and flow in the stir zone in FSW process. This creates an importance on the analytical, numerical and computational modelling of friction stir welding. In this review on friction stir welding, special focus is given on various analytical models developed to estimate peak temperature during the process. The different approaches that have been used to investigate heat generation are presented and their drawbacks are discussed. Assumptions made in the modelling and their corresponding effects in the results are also addressed.

KEYWORDS: Friction Stir Welding, Thermal Modelling & Thermo Mechanical Modelling

Received: Nov 27, 2018; **Accepted:** Dec 17, 2018; **Published:** Jan 03, 2019; **Paper Id.:** IJMPERDFEB201918

Original Article

INTRODUCTION

Friction Stir Welding (FSW) is one of the metal joining processes, performed in plasticised solid state parental metal with the help of frictional heat. In a metal joining, the weld properties are influenced by the peak temperature during the process and rate of cooling after the joining process [1]. FSW produces comparatively better weld properties as it is performed in much lower temperature than other conventional joining processes [2]. This solid state metal joining process is performed by forcing a non-consumable rotating tool to penetrate and move through the entire joint of the parts to be welded (Figure.1). All the welding parameters in FSW are selected to soften the work piece material to facilitate mechanical deformation. The frictional heat produced in the tool/matrix interface plasticises and joins the parental metal in the line of joint and the tool [3].

FSW operations can be divided into several phases based on the relative motion absorbed between work piece and tool [5]. Initially tool pin is rotated and allowed to pierce vertically into the work piece called plunging operation and the material is too cool for plastic deformation. In this stage, rubbing action created by the pin creates chips like other machining process and temperature is increased. When the tool shoulder touches the weld surface the vertical movement is stopped and tool is allowed to rotate for a while called dwell period. The entire tool shoulder and pin surface contribute to the frictional heating and the work piece reaches a critical temperature for plastic flow. After these two, welding operation is carried out by the horizontal movement of the welding tool along the joint line. Most of the welding defects like porosity and void formation in the conventional joining processes are eradicated in FSW as the shoulder confines the underlying material. During the plunge action, the

conical shoulder acts like an escape volume of the material displaced by the tool pin [6].

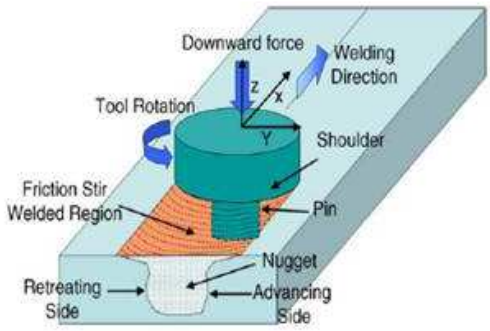

Figure 1: Different Phases in Friction Stir Welding Process [4]

Almost all the properties of the final weld depend on generating heat and heat flow through it during the joining process [7]. So understanding the temperature profile during the process is important to optimise the weld tool geometry and other weld parameters in order to obtain improved weld microstructure and other mechanical properties associated with it.

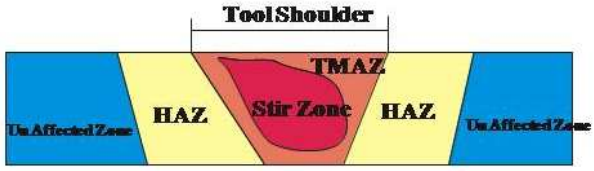

Figure 2: Different Zones in the FSW Process [4]

This thermo mechanical stir metal joining process produces two different zones namely stir zone and heat affected zone (Figure.2). Intense deformation produced by the FSW tool rotation makes all conventional temperature measurement techniques like embedding thermocouples in the stir zone impossible [8]. This necessitates an analytical thermal modelling to predict generated heat to define thermal profile during friction stir welding process. Therefore the maximum temperature is estimated indirectly by analysing the change in the microstructure like the dissolution of larger precipitates [9] in the stir zone of the weld or by measuring the temperature in the region adjacent to the stir zone with the help of embedded thermocouples and predicting the peak temperature in the stir zone by analytical methods as the temperature is a function of distance [10]. These indirect estimations couldn't produce the promising result as sometimes the predicted temperatures are more than melting point [11] which is not true in FSW as it is a solid state joining process. This is due to the fact that this increase in the dislocation density and an increase in the amount of the grain surface and grain edge per unit volume is not only because of a temperature rise, but also due to the plastic deformation produced by the tool during stirring action [12].

In FSW, heat is generated by the friction developed in the tool workpiece interface and also due to the plastic deformation that occurs away from the tool workpiece interface. Local heat generation produced by the deformation and grain boundary sliding contributes only 4.4% of the total heat produced [13] and the remaining heat generation is because of frictional heat. So in this paper, special emphasis has been given on the analytical estimation of heat generation due to the friction in the tool/matrix interface.

THERMAL MODELLING

Thermal modelling is used to analyse temperature distribution during FSW. All thermal models in FSW are interested to solve a general heat conduction equation (1), by opting different initial condition and appropriate boundary conditions [14].

$$\rho C_p \dot{T} + \mu_i \rho C_p T_{,i} = (kT_{,i})_{,i} + \frac{Q_{gen}}{V} \quad (1)$$

Here Q_{gen}/V denotes volumetric heat source. Unlike other joining process, in FSW heat is generated not only by means of external sources, but also generated by friction and plastic dissipation in the tool/matrix interface [15]. Tang et al.[16] analysed the tool shoulder and the tool pin's contribution to the heat generation and concluded that as the shoulder has contact area and contact pressure comparatively much higher than the pin, shoulder dominates the heat generation. Assuming only sliding condition and heat generation by the shoulder in the interface, a simplified expression for heat generation (eqn2) is derived by implementing numerical model based on position dependent surface flux for flat shoulder FSW tool neglecting the heat generated by the pin[17].

$$q_{total} = \frac{3Q_{total}r}{2\pi R^3_{shoulder}} \quad (2)$$

This is a commonly used expression to calculate heat generation. In this equation Q_{total} is an input parameter. Unlike other metal joining process, Q_{total} is not controlled by external sources. But it itself depends on internal function variables. So this equation has limitations and cannot be used to predict all FSW welding parameters. For example, Q_{total} itself is a function of rotational speed [18]. In most of the thermal modelling, Q_{total} is measured using dynamometer and is taken as a constant to find q_{total}[19].

Thermal model is used to analyse temperature distribution. In FSW, as generated heat is a function of frictional contact conditions and material flow it cannot be a constant value [20]. Heat generation also depends on tool geometry and other weld parameters [18]. So pure thermal model has limitations and is replaced by thermo mechanical or CFD model which couples heat generation and material flow by plastic dissipation in the shear layer and frictional contact at the tool and work piece [21].

THERMAL MODELING BASED ON THE SOLIDUS TEMPERATURE

It was observed from the various experimental analysis [22-25] that peak temperature during FSW lies between 60 to 90% of the solidus temperature of parental metal. Arbegast and Hartley [26] derived an expression (eqn3) which relates the peak temperature developed during the process and solidus temperature of the parental metal.

$$\frac{T}{T_m} = \left(\frac{\omega^2}{V\ X\ 10^4}\right)^{\alpha} \quad (3)$$

where α is in the range of 0.04 to 0.06, k is the thermal conductivity, ω and V are tool rotation and traverse speed.

During the joining process if the generated temperature approaches solidus temperature of the material to be joined, the material in the tool metal interface will act like a fluid, which reduces friction in the tool metal contact surface tremendously and results ina negligible heat generation and temperature brought down. This self-stabilizing effect always maintains the temperature below its solidus temperature [26]. In an approach developed by Tutum et al.[27] peak temperature in the tool metal interface is taken as a constraint to optimize other weld parameters. This approach helps to

model temperature profile without prior knowledge about heat input. A thermal model developed based on this assumptions deviates from actual conditions as the peak temperature is not constant throughout the process. Varying temperature during the process produces a non-uniform thermo mechanical conditions which are not considered in this thermal modelling. A new thermo pseudo mechanical formulation can overcome these limitations which consider the varying conditions in the prediction of heat generation [28].

THERMO PSEUDOMECHANICAL MODELLING

In this approach, the total amount of heat generation is modelled from frictional heat and heat developed due to the plastic dissipation at the tool metal interface [17-19]. Colomb's law of friction is used to determine the shear stress between the contact surfaces (eqn4). A uniform thickness shear layer was prescribed analytically. The material flow in the shear layer produces convective heat generation in the weldment, around the probe.

$$\tau = \mu P = \mu\sigma \tag{4}$$

Hasimoto et al.[29] observed that the peak temperature during FSW is a strong function of tool traverse and rotation speed. Based on the influence of contact pressure and tool rotation rate, Friggard et al[30] developed a model (eqn5)to calculate heat input per unit area as

$$q_0 = \frac{4}{3}\pi^2 \mu P \omega R^3 \tag{5}$$

Where μ is friction coefficient, P is contact pressure, ω angular velocity of tool and R is radius of tool shoulder.

Heat generation due to the friction is the product of the tangential speed of the tool with respect to the workpiece at the tool work piece interface and the frictional force and given by (eqn6)[31],

$$dQ = (\omega r - V\sin\theta)\mu p dA \tag{6}$$

Where p is local pressure and d A is element area.

Normally heat is generated in the surface very close to the tool and has a complex geometry based on the tool geometry. But for analytical estimation, tool design is assumed to be conical shoulder with a cone angle α or for flat shoulder surface in which α = 0. Vsinθ can be neglected as the effect of tool rotation speed (ωr) is much higher than the effect of tool traverse speed (Vsinθ) [32&33] so heat generation equation can be simplified as (en7)

$$dQ = \omega dM = \omega r dF = \omega r \tau_{contact} dA \tag{7}$$

In equation (7), for dA is achieved considering circular surface perpendicular to the rotation axis for probe tip, cylindrical surface parallel to the rotation axis for probe side and conical surface tilted with respect to the rotation axis (Figure.3).

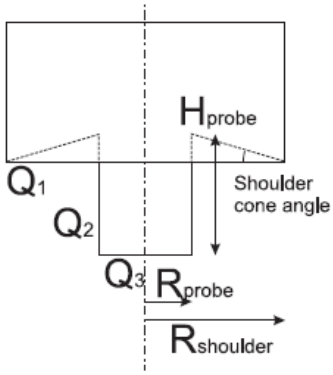

Figure 3: Heat Generation Contributions in Analytical Estimation [36]

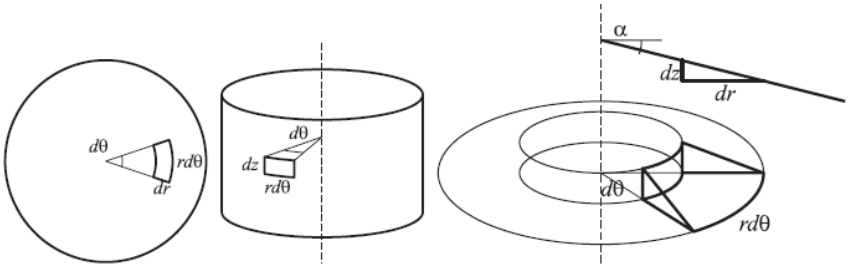

Figure 4: A Schematic Drawing of Surface Orientations and Infinitesimal Segment Areas for Probe Tip, Probe Side and Conical Tool Shoulder [36]

Total heat generated is an addition of heat generated under the tool shoulder (Q_1), tool probe aside (Q_2) and probe tip (Q_3) (Figure 4). Heat generation equations for Q_1,Q_2 and Q_3 are derived from general heat generation equation[34]. Adding all final equation derived is (eqn8).

$$Q_{total} = \frac{2}{3}\pi\tau_{contact}\omega(R^3_{shoulder} + 3R^2_{probe}H_{probe}) \quad (8)$$

In this equation shear stress value is kept constant in the contact interface. But in reality, the contact shear stress varies depending on contact conditions [35]. To define contact yield stress, three different fully sticking, fully sliding and partial sticking/sliding contact conditions have to be analysed in the tool/matrix interface [37].

Sticking Condition

The work piece is divided as surface segment and lower surface segment. If the shear yield stress due to the frictional contact between the tool and the work piece is more than the yield stress of the underlying segment, it results in full sticking condition. In this condition, the matrix segment accelerates till internal matrix shear stress and contact shear stress become equal and finally reaches tool velocity. Schmidt et al [36] defined a contact state variable (δ) (eqn9) as

$$\delta = \frac{V_{matrix}}{V_{tool}} = 1 - \frac{\dot{\gamma}}{V_{tool}} \quad (9)$$

where $\dot{\gamma}$= slip rate and $V_{tool} = r\omega$.

During sticking condition ($\delta = 1$ (or) $V_{tool} = V_{matrix}$). Shear stress occurs in the layer very close to the tool/matrix interface. In this case, there exists a change in velocity from the layer sticking with the tool till the stationary layer in the matrix. So the deformed layer starting from the tool interface should be treated as a shear surface. So shear stress $\tau_{contact} = \tau_{yield} = \sigma_{yield}/\sqrt{3}$. The extent of slip can also be estimated by experimentally measured values using the expression (eqn10)

given by Deng et al [38].

$$\delta = 0.2 + 0.8\left[1 - exp\left(-\delta_0 \frac{\omega r}{\omega_0 R_s}\right)\right] \quad (10)$$

Where ω r represents the torque at the point of calculation and $\omega_0 R_s$ is the maximum torque that can be produced by the tool.

Sliding Condition

Sliding condition occurs when friction shear stress is lesser than internal matrix yield stress. In this condition matrix segment slightly elastically deforms and shear stress is equal to the dynamic contact shear stress. During fully sliding condition (δ = 0 (or) $V_{matrix} = 0$). Shear stress occurs in the contact interface. Here $\tau_{contact} = \tau_{friction} = \mu P = \mu\sigma$. Here P and σ are contact pressure. In a thermal model developed by Hilgert et al.[39] pure sliding condition is adopted and heat generation equation is simplified as, $q_{total} = \omega_{tool}\, r\, \tau_{yield}$.

Partial Sticking/Sliding Condition

In this contact shear stress is equal to the internal matrix yield stress due to a quasi-stationary plastic deformation rate. The matrix segment accelerates and stabilises in a velocity lesser than the tool surface velocity n a new approach, Schmidt et al.[19] derived an equation (eqn11) considering frictional and plastic dissipative heating under varying contact yield stress.

$$q_{total} = \dot{\gamma}\tau_{friction} + (\omega_{tool} r - \dot{\gamma})\tau_{yield} \quad (11)$$

where q_{total} is the total heat flow,$\dot{\gamma}$ is the shear rate, $\tau_{friction}$ is the shear stress due to friction, τ_{yield} is shear yield stress, ω_{tool} is the angular velocity of the tool and r is the distance from the heat source to the centre.

An energy dependent expression developed by Hamilton et al. [40] reveals thatslip

$$\delta_E = exp\left(-\frac{(E_l)_{eff}}{(E_l)_{max}}\right) \quad (12)$$

when $(E_l)_{eff} = 0$ then $\delta_E = 1$ and sticking friction dominates. When $(E_l)_{eff}$ increases, metal in the tool/metal interface softens and slip occurs. So maximum possible case can be $(E_l)_{eff} = (E_l)_{max}$ and in this case $\delta_E = 0.37$. From this it can be concluded that slip rate can lies between1 to 0.37.

EXPERIMENTALLY FOUND TORQUE BASED THERMO PSEUDOMECHANICAL MODELING

In the modelling of temperature profiles Rosenthal solution is used. The input power during friction stir welding process has been used as input in the various models [41, 42] developed based on Rosenthal equation. Khandkar et al. [43] developed heat input models based on torque input as the heat input is equal to the rotational power. This experimentally arrived torque value replaces the heat input to find yield stress on the contact surface in the elevated temperature. This analytical solution created a link between plunge force and heat generation as the plunge force is used to calculate torque input.

$$T_{total} = 2\mu F\left(\frac{r_0}{3} + \frac{r_i^2}{r_0^2} h\right) \quad (13)$$

where F is applied force, r_0 is shoulder radius, r_i is radius of pin and h is pin height. The obtained analytical results

compared with experimental obtained by Frigaard et al [44 &4 5] (Figure 5) to analyse the relationship between plunge force and heat generation.

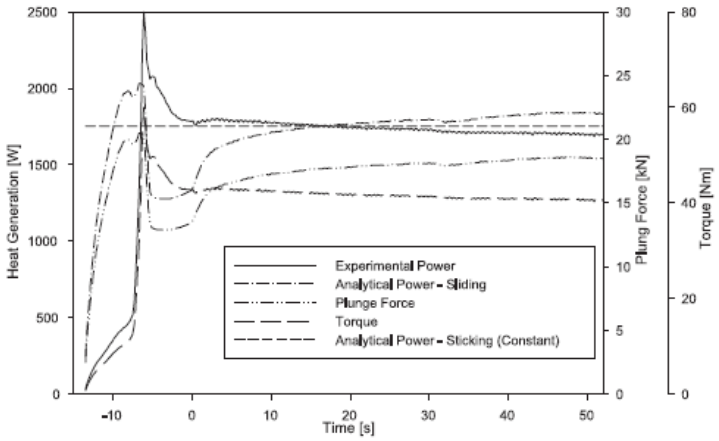

Figure 5: Comparison of Plunge Force Experienced [44]

During plunge period, plunge force and torque increases steadily. During dwell, in analytical solution it is predicted to be sliding and uniform pressure condition. But from the experimental values it is observed that plunge force and torque reduces. During welding period, little increase in the plunge force, but torque remains the same. Thus an increase in the plunge force does not affect torque. It is understood that during welding, a reaction force is developed which opposes plunge force and tries to move the tool upwards. To overcome the reaction force, the machine gives extra force. Thus at this stage, plunge force cannot be used to access the heat generation.

Power input given to the machine is influenced by tool rotation speed (ω) and tool transverse speed (v) [46] and is given by

$$P_{tool} = M\,\omega + F_x\,V \tag{14}$$

Where F_x is forward force, M denotes torque. The relationship between torque, tool rotation speed and tool traverse speed is analysed [47 &48] and it was concluded that torque could be reduced by the increase in tool rotation and reduce in tool traverse speed. The influence of tool rotation speed is higher than tool traverse speed. Based on this an equation was developed by L . Cui et al. [15] which relates the input power and tool rotation speed

$$M = M_0 + M_f\, e^{-n\omega} \tag{15}$$

where M_0 is the minimum torque required, M_f is the pre exponential parameter and n denotes the decay parameter. Upadhyay and Reynold's [41] study on Peak temperature (T) during FSW with respect to tool rotation (ω) reveals that T is a function of ω and they expressed peak temperature, based on the graph drawn between T and ω, as

$$T = T_0 + T_f\,(1-e^{-q\omega}) \tag{16}$$

THERMO PSEUDOMECHANICAL MODELING CONSIDERING SURFACE FLUX

Yield stress in the shear layer is independent of pressure. But it is highly influenced by temperature. In the previous models used to find heat generation, in order to apply constant shear yield stress, an isothermal is assumed in the tool/matrix interface. But in real practice, heat generation depends on temperature, strain and strain rate [19]. To overcome this, a temperature dependent heat generation is derived as a surface flux and given by, $q_{total} = \omega r\tau(T)$.

Here T = T(X, Y&Z) and treated as non-uniform at the tool/matrix interface. This model is compared with the previous linearly dependent heat generation model in which heat generation is not dependent on temperature (Figure 6) [19].

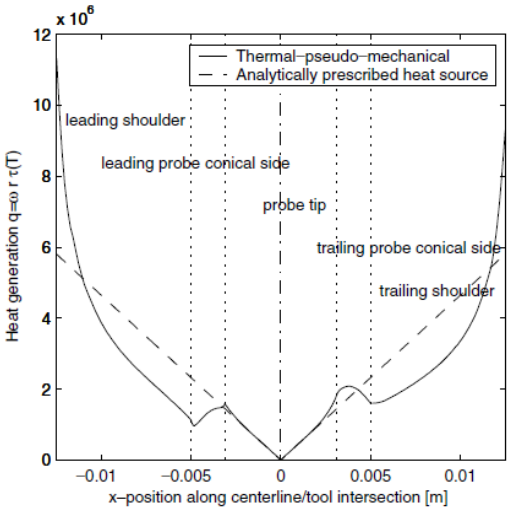

Figure 6: Linear Heat Generation Vs Temperature Dependent Heat Generation Model [19]

It was observed in the probe tip that the generated heat is same in both the cases as there is no change in the temperature. But in the leading and trailing shoulder region, q(T) is exponentially increasing. This reveals that there is an increase in yield stress due to the decrease in temperature for larger radii.

CONCLUSIONS

The amount of heat generation in FSW depends on so many parameters like, tool rotation and traverse velocity, tool, tilt angle, axial force, friction coefficient, shear stress, duration of welding etc. The mutual dependence and influence of all these parameters make the analytical modelling complicated. It is quite impossible to consider all and normally the most important dependences are only considered in the analytical modelling. In order to improve the accuracy of the analytical modelling it should not rely only on analytical algebra, but also on numerical calculations and implementation of experimentally obtained variables. For example, implementation of a numerical flow model and usage of experimentally estimated friction coefficient and thermal conductivity in the analytical model gives a precise result.

Most of the analytical modelling considers a uniform heat generation in the tool shoulder metal interface. But the frictional heat generation depends on the coefficient of friction between the surfaces in contact and surface velocity, which are not constant and but increasing gradually from the centre point to the tool shoulder edge and this leads to the non-uniform heat generation from the centre to the shoulder edge.

The difference in the recorded hardness in the heat affected zone on the advancing side and retreating sides reveals asymmetry in the distribution of heat due to the change of direction of tool rotation. In order to simplify problems, many thermal models assume the symmetric condition on both the sides causing deviation from the experimentally measured values. In spite of all these assumptions and its drawbacks in the analytical modelling, it helps to have a clear physical understanding of the process and to predict the temperature profile on various stages so that the process parameters can be easily optimised.

REFERENCES

1. *Yihua Xiao, Heifeizhan, YuantongGu, Qinghua Li, Modeling heat transfer during friction stir welding using meshless particle method, International journal of Heat and mass Transfer, Vol 104, (2017) 288-300.*
2. *Suresh D. Meshram, Archana G. Paradkar, G. Madhusudhan Reddy, Sunil Pandey, Friction stir welding: An alternative to fusion welding for better stress corrosion cracking resistance of maraging steel, Journal of Manufacturing Processes, Volume 25, January 2017, Pages 94–103*
3. *S Guerdoux and L Fourment, A 3D numerical simulation of different phases of friction stir welding, Modeling and Simulation in Materials Science and Engineering, (2009) Volume 17, Number 7*
4. *S.Sattari, H.Bisadi, M.sajed, Mechanical Properties and Temperature Distributions of Thin Friction Stir Welding Sheets of AA5083, International Journal of Mechanics and Applications, (2012); 2(1): 1-6*
5. *L. Shi, C.S. Wu, Transient model of heat transfer and material flow at different stages of friction stir welding process, Journal of Manufacturing Processes, Volume 25, January 2017, Pages 323–339*
6. *Suresh D.Meshram, Archana G. Paradkar, G.Madhusudhan Reddy, Sunil Pandey, Friction stir welding: An alternative to fusion welding for better corrosion cracking resistance of maraging steel, Journal of manufacturing processes, 25(2017) 94-103.*
7. *H. Su, C.S. Wu, A. Pittner, M. Rethmeier, Thermal energy generation and distribution in friction stir welding of aluminum alloys, Volume 77, 1 December 2014, Pages 720–731*
8. *Panneerselvam, K., & Lenin, K. (2013). Study on hardness and micro structural characterization of the friction stir welded Nylon 6 plate. Int J Mech Eng, 2, 51-62.*
9. *Jingming Tang, yifushen, Numerical simulation and experimental investigation of friction stir lap welding between aluminium alloys AA2024 and AA7075, Journal of Alloys and compounds(2016), doi:10.1016/j.jallcom.2016.01.138*
10. *Y.S. Sato, H. Kokawa, M. Enmoto, S. Jogan, Microstructural evolution of 6063 alluminium during friction stir welding, Metallurgical and Material Transactions. A 30 (1999) 2429 - 2437.*
11. *M.W. Mahoney, C.G. Rhodes, J.G. Flintoff, R.A. Spurling, W.H. Bingel, properties of friction stir welded 7075-T651, Metallurgical and Material Transactions. A 29 (1998) 1955.*
12. *Mishra RS, Ma ZY. Friction stir welding and processing. Material Science and Engineering, R2005;50:1–78.*
13. *Zhu Q, Sellars CM, Bhadeshia HKDH. Quantitative metallography of deformed grains. Material Science Technology 2007;23(7):757–66.*
14. *Bastier A, Maitournam MH, van Dang K, Roger F. Steady state thermomechanicalmodeling of friction stir welding, Science and Technology of Welding and joining, 2006;11:278-88.*
15. *M.Song, R.kovacevic, Thermal modeling of friction stir welding in a moving coordinate system and validation, International Journal of Machine Tools & manufacture 43(2003) 605-615.*
16. *L. Shi, C.S. Wu, H.J. Liu, The effect of the welding parameters and tool size on the thermal process and tool torque in reverse dual-rotation friction stir welding, International Journal of Machine Tools and Manufacture, Volume 91, April 2015, Pages 1–11.*
17. *W. Tang, X. Guo, J.C. McClure, L.E. Murr, J. Heat input and temperature distribution in friction stir welding, Journal of material processing and manufacturing science, 7 (1998) 163.*

18. *H. Schmidt, J. Hattel, An analytical model for heat generation in Friction Stir Welding, Science and Technology of Welding and joining 10(2005) 2.*

19. *TanmoyMedhi, BarnikSaha Roy, SubodhDebbarma, S.C. Saha, Thermal modeling and effect of process parameters in friction stir welding, 4th International Conference on Materials Processing and Characterzation, Volume 2, Issues 4–5, 2015, Pages 3178-3187*

20. *H.B.Schmidt and J.H.Hattel, Thermal modeling of friction stir welding, ScriptaMaterialia 58 (2008) 332-337*

21. *Xiaocong He, FengshouGu, Andrew Ball, A review of Numerical analysis of Friction Stir welding, Progress in Material Science 65 (2014), 1-66*

22. *Gao-qiang Chen, Qing-yu Shi,, Yu-jia Li, Yan-jun Sun, Qi-lei Dai, Jin-yaoJia, Yu-can hu, Jian-jun Wu, Computational fluid dynamics studies on heat generation during friction stir welding of aluminum alloy, Computational Materials Science, Volume 79,*

23. *Rajamanickam N, Balusamy V, Madhusudhanna Reddy G, Natarajan K. Effect of process parameters on thermal history and mechanical properties of friction stir welds. Mater Des 2009;30:2726–31.*

24. *Cerri E, Leo P. Warm and room temperature deformation of friction stir welded thin aluminium sheets. Mater Des 2010;31:1392–402.*

25. *M.J.Peel, A.Steuwer, P.J.Withers, T.Dickerson, Q.Shi, H.Shercliff, Dissimilar friction stirweldsinAA5083-AA6082.Part1:process parameter effectson thermal history and weld properties, Metallurgical and Materials Transactions A37(2006)2183–2193.*

26. *J.Yan, M.A.Sutton, A.P.Reynolds, Process structure property relationships for nugget and heat affected zone regions of AA2524-T351 friction stir welds, Science and Technology of Welding and Joining 10(2005)725–736.*

27. *Yunus, M. O. H. A. M. M. E. D., & Alsoufi, M. S. (2015). A statistical analysis of joint strength of dissimilar aluminium alloys formed by friction stir welding using taguchi design approach, anova for the optimization of process parameters. IMPACT: Int J Res Eng Tech (IMPACT: IJRET), 3(7), 63-70.*

28. *W.J. Arbegast, P.J. Hartley, in: Proceedings of the Fifth International Conference on Trends in Welding Research, Pine Mountain, GA, USA, June 1–5, 1998, p. 541.*

29. *C.C. Tutum, H. Schmidt, J. Hattel. M.P. Bendsøe, Proceedings of the Seventh World Congress on Structuraland Multidisciplinary Optimization, Seoul, 2007, pp.2639–2646.*

30. *Lai-zhijin, Rolf sandstorm, Numerical simulation of residual stresses for friction stir welds in copper canisters, Journal of Manufacturing Processes 14 (2012) 71-81.*

31. *T. Hashimoto, S. Jyogan, K. Nakata, Y.G. Kim, M. Ushio, in: Proceedings of the First International Symposium on Friction Stir Welding, Thousand Oaks, CA, USA, June 14–16, 1999.*

32. *O. Frigaad, O. Grong, O.T. Midling, A process model for friction stir welding of age hardening alluminumalloys,Journal of Metallurgical and Materials Transactions. A 32 (2001) 1189.*

33. *Nandan R, DebRoy T, Bhadeshia HKDH. Recent advances in friction-stirwelding-process, weldment structure and properties. Progress in Mater Science 2008;53:980–1023.*

34. *Chen CM, Kovacevic R. Finite element modeling of friction stir welding – thermal and thermomechanical analysis. International Journal of Machine Tools &Manufacture 2003;43:1319–1326.*

35. *Darwins, A. K., & Satheesh, M. (2017). Effect Of Friction Stir Welding Process on Mechanical Properties and Microstructure of ZE42 Magnesium Alloy.*
36. *Zhang HW, Zhang Z, Chen JT. Finite element simulation of the friction stir welding process. Material Science and Engineerng A 2005;403:340–8.*
37. *Y.J. Chao, X. Qi, W. Tang, Heat transfer in friction stir welding- experimental and numerical studies, Journal of Manufacturing and Engineering. 125 (2003).*
38. *Q. Shi, T. Dickerson, H. Shercliff, in: Proceedings of the Fourth International Symposium on Friction Stir Welding, Park City, UT, 2003.*
39. *H. Schmidt, J. Hattel, J. Wert, A local model for the thermomechanical conditions in friction stir welding, Journal of modeling and simulations in material science engineering. 12 (2004).*
40. *Subrata pal, M.P.Phaniraj, Determination of heat partition between tool and workpiece during FSW of SS304 using 3D CFD modeling, Journal of Materials processing Technology, volume 222, (2015), 280 – 286.*
41. *Deng Z, Lovell MR, Tagavi KA. Influence of material properties and forming velocity on the interfacial slip characteristics of cross wedge rolling. ManufacturingScienceEngineerng 2001;123:647–53.*
42. *J. Hilgerta, H.N.B. Schmidtb, J.F. dos Santosa, N. Hubera, Thermal models for bobbin tool friction stir welding, Journal of Materials Processing Technology, 211(2011) 197-204.*
43. *C.Hamilton, S.Dymek, A Sommers, A thermal model of friction stir welding in aluminium alloys, International journal of Machine Tools & Manufacture 48 (2008) 1120-1130*
44. *P. Upadhyay, A.P. Reynolds, Effects of thermal boundary conditions in friction stir welded AA7050-T7, Materials Science and Engineering A 527 (2010) 1537–1543.*
45. *K.J. Colligan, A proposed conceptual model of the process variables related to heat generation in friction stir welding of aluminium, in: Proceedings of the Seventh International Symposium of Friction Stir Welding, Japan, TWI, 2008.*
46. *Khandkar M Z H, Khan J A and Reynolds A P, Prediction of temperature distribution and thermal history during Friction Stir Welding: Input torque based model, 2003, Science and technology of welding and joining. 8 165–74.*
47. *Frigaard, Grong and Midling T, A process model for friction stir welding of age hardening aluminium alloys,2001 Metallurgical and Materials Transactions. A 32 1189–200*
48. *Frigaard Ø, Grong Ø, Bjørneklett B and Midling O T 1999 1st Int. Symp. on Friction Stir Welding (Thousand Oaks, CA)*
49. *P. Kalya, K. Krishnamurthy, R.S. Mishra, J.A. Baumann, Specific energy and temperature mechanistic models for friction stir processing of Al-F357, in: R.S. Mishra, M.W. Mahoney, T. Lienert, K.V. Jata (Eds.), Friction Stir Welding and Processing IV, TMS2007, 113–125.*
50. *K.J. Colligan, R.S. Mishra, A conceptual model for the process variables related to heat generation in friction stir welding of aluminium, ScriptaMaterialia, 58 (2008) 327–331.*
51. *A. Arora, R. Nandan, A.P. Reynolds, T. Debroy, Torque, power requirement and stir zone geometry in friction stir welding through modeling and experiments, ScriptaMaterialia, 60 (2009) 13–16.*